

Lorentz Forces in the Container

K. Horáková, K. Fraňa

Abstract—Leading topic of this article is description of Lorentz forces in the container with cuboid and cylindrical shape. Inside of the container is an electrically conductive melt. This melt is driven by rotating magnetic field. Input data for comparing Lorentz forces in the container with cuboid shape were obtained from the computing program NS-FEM3D, which uses DDS method of computing. Values of Lorentz forces for container with cylindrical shape were obtained from inferred analytical formula.

Keywords—Lorentz forces, magnetohydrodynamics, rotating magnetic field, computing program NS-FEM3D

I. INTRODUCTION

MAGNETOHYDRODYNAMICS (MHD for short) is a theory of interaction between magnetic field and moving, conducting fluids [1]. First mentions regarding MHD appeared in relation to astrophysics and geophysics. In the fifties the interest in MHD focused especially to plasma physics and thermonuclear fusion control. The interest in MHD was extended to industry later.

Using of the rotating magnetic field (RMF) is mostly surveyed in recent years. In a few papers were compared static and rotating magnetic fields [2]. The rotating magnetic field was turned out like better usable. In next papers the flow stability and formation instabilities were monitored [3]. In the work of Dold a Benze [2] the experimental reduction of the temperature fluctuations in the case of crystal growth was described. RMF is testing for using gallium and for different metallographic technics (Float Zone, Czochralski, Bringham nebo Travelling Heater Method) [4, etc]. Production of semiconductors is another possibility of using magnetic field [5], [6]. Magnetic field is exploited also in magnetic damping, levitation melting etc. [7], [1].

The subject of this work is a description of the melt flow inside of the container. The flow of the melt is driven by rotating magnetic field. In Navier-Stokes equations for flow calculations there are occurred the external forces. In the flow of melt driven by a rotating magnetic field these forces are the Lorentz forces. Theme of first part this article is short determination of analytical formula of cylindrical container

Lorentz forces (for more details see to my earlier works [8], [9]). The second part of this article is comparing Lorentz forces contours of cylindrical container (analytical formula) with Lorentz forces in the container with cuboid shape. Data of Lorentz forces in cuboid container are obtained from the computing program NS-FEM3D [10], which uses DDS method of computing. From this computing program are obtained database of value Lorentz forces for different Taylor numbers.

II. LORENTZ FORCES IN THE CONTAINER IN CYLINDRICAL SHAPE

A. Determination of analytical formula of Lorentz forces

The container is considered with electrically isolated walls, the melt inside the container is conductive with density ρ , kinematic viscosity ν and electric conductivity σ . Flow of the melt is driven by rotating magnetic field with magnetic induction B (noted in the cylindrical coordinates):

$$B = B_0 \cdot \sin(\varphi - \varpi \cdot t) \cdot \mathbf{e}_r + B_0 \cdot \cos(\varphi - \varpi \cdot t) \cdot \mathbf{e}_\varphi \quad (1)$$

In this formula (1) \mathbf{e}_r and \mathbf{e}_φ are unit vectors in radial and azimuthal direction and ϖ is the constant angular frequency of the field.

Magnetic induction has only components B_r a B_φ because is assumed that vertical size of bipolar inductor is bigger than the height of the melt in the container. Vector potential A was determined with $\mathbf{B} = \nabla \times \mathbf{A} = \text{rot } \mathbf{A}$,

$$\text{thus: } \mathbf{A} = -B_0 \cdot r \cdot \cos(\varphi - \varpi \cdot t) \cdot \mathbf{e}_z. \quad (2)$$

The electric field intensity could be computed by this vector potential (2):

$$\mathbf{E} = -(\nabla \Phi_{\text{rot}} + \frac{\partial \mathbf{A}}{\partial t}),$$

$$\text{thus } \mathbf{E} = -\nabla \Phi_{\text{rot}} + B_0 \cdot r \cdot \varpi \cdot \sin(\varphi - \varpi \cdot t) \cdot \mathbf{e}_z \quad (3)$$

Equation (1) is valid for inductor without material inside. If some material with high electric conductivity (powerful to affect the magnetic field) is inserted inside the inductor, this magnetic field will be changed by skin-effect. For that reason non-dimensional frequency K is monitored.

$$K = \mu \cdot \sigma \cdot \varpi \cdot R^2 \quad (4)$$

where μ is magnetic permeability, σ is electric conductivity and ϖ is magnetic field angular velocity. If non-dimensional frequency $K \ll 1$, magnetic field (1) penetrates by whole volume of the melt without change and rotating variables rotating with the same frequency. In this case of $K \ll 1$ the scalar potential $\Phi_{\text{rot}}(r, \varphi, z, t)$ is possible to separate to two parts [11],

K. Horáková is with the The Faculty of Mechanical Engineering of Technical University of Liberec, Department of Power Engineering Equipment, Liberec, Czech Republic (phone: 00420 48 535 3434; e-mail: katerina_horakova@centrum.cz).

K. Fraňa, is with the The Faculty of Mechanical Engineering of Technical University of Liberec, Department of Power Engineering Equipment, Liberec, Czech Republic (phone: 00420 48 535 3436; e-mail: karel.frana@seznam.cz).

This work was financially supported by the research project MSM 4674788501

$$\Phi_{rot}(r, \varphi, z, t) = \Phi_1(r, z) \cdot \sin(\varphi - \varpi \cdot t) + \Phi_2(r, z) \cdot \cos(\varphi - \varpi \cdot t) \quad (5)$$

Current density j is determined with $\mathbf{j} = \sigma(\mathbf{E} + \mathbf{v} \times \mathbf{B})$ (6) Because of low-induction and low-frequency it is possible to use some simplification for calculation current density j . The magnetic field affects that the melt moves. But the melt does not affect magnetic field by return (or very small). The cross product term of the flow velocity and the magnetic induction could be neglected (flow angular velocity is much lower than magnetic field angular velocity) and reduced Ohm's law is:

$$\mathbf{j} = \sigma \cdot \mathbf{E} \Rightarrow \mathbf{j} = \sigma \cdot \left(-\frac{\partial \Phi_{rot}}{\partial r} \cdot \mathbf{e}_r - \frac{1}{r} \frac{\partial \Phi_{rot}}{\partial \varphi} \cdot \mathbf{e}_\varphi - \frac{\partial \Phi_{rot}}{\partial z} \cdot \mathbf{e}_z + B_0 \cdot r \cdot \varpi \cdot \sin(\varphi - \varpi \cdot t) \cdot \mathbf{e}_z \right) \quad (7)$$

where σ is the melt electric conductivity.

Using of equation $\nabla \cdot \mathbf{j} = \text{div } \mathbf{j} = 0$ is possible to get equation:

$$\left(\nabla^2 - \frac{1}{r^2} \right) \cdot \Phi_1 = 0. \quad (8)$$

Solution of (8) is difficult because scalar potential Φ_1 is bivariate function (r, z) . Solution of Φ_2 is after some computing zero. This equation (8) could be solved by the Fourier method of a variable separation and then solving two separate differential equations. The part which has the dependence only on the variable r is converted to the shape of Bessel differential equations and then solved by Bessel functions. The second part which has the dependence only on the variable z is differential equation of the second order with constant coefficient and this equation is solved by the characteristic equation (for more details see to my earlier works [8], [9]).

After some mathematical manipulations and solving boundary conditions the final analytical formula of scalar potential:

$$\Phi(r, z) = \sum_{i=1}^{\infty} \frac{2 \cdot J_1(m_i \cdot r)}{m_i \cdot (m_i^2 - 1) \cdot J_1(m_i)} \cdot \frac{\cosh(m_i \cdot z) - \cosh(m_i \cdot (H - z))}{\sinh(m_i \cdot H)} \quad (9)$$

where m are roots of the equation $J_1'(m) = 0$, z is non-dimensional height of the container, r is non-dimensional radius of the container, H is non-dimensional total height of the container and J_1 is Bessel function of the first kind. This equation corresponds to the published results of other authors see [12].

Lorentz forces are solved by formula: $\mathbf{f}_{rot} = \mathbf{j}_{rot} \times \mathbf{B}_{rot}$.

(10) After that result are the Lorentz forces time-averaged over one period (2π) .

$$\overline{\mathbf{f}_{rot}} = \frac{1}{2 \cdot \pi} \cdot \int_0^{2\pi} \mathbf{f}_{rot} d\varpi t \quad (11)$$

The final formula of time-averaged Lorentz forces in azimuthal direction is in this form:

$$\overline{\mathbf{f}_{rot \varphi}} = \frac{\sigma \cdot B_0^2 \cdot \varpi \cdot r}{2} \cdot \left(1 - \frac{2}{r} \sum_{i=1}^{\infty} \frac{J_1(m_i \cdot r)}{(m_i^2 - 1) \cdot J_1(m_i)} \cdot \frac{\sinh(m_i \cdot z) + \sinh(m_i \cdot (H - z))}{\sinh(m_i \cdot H)} \right) \quad (12)$$

This equation corresponds to the published results of other authors as well, see [12]. Forces in the radial and axial direction are zero in this simplification.

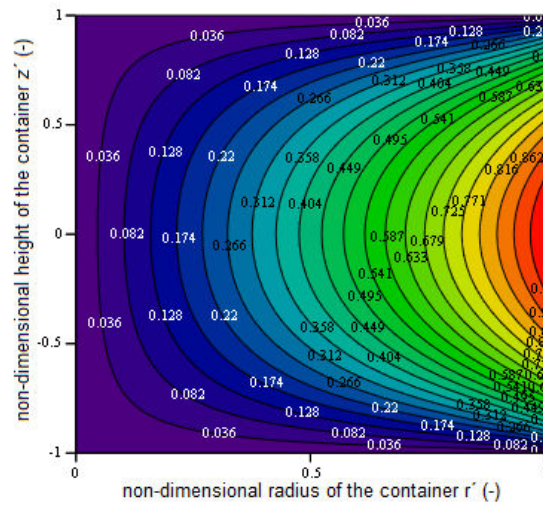


Fig. 1 Contours of time-averaged Lorentz forces in azimuthal direction for cylindrical container

B. Contours of Lorentz forces

Fig. 1 shows contours of time-averaged Lorentz forces in azimuthal direction. In horizontal axis non-dimensional radius of the cylinder (container) $r'(-)$ is used. That means radius $r(m)$ was divided by magnitude of container radius R . In vertical axis non-dimensional height of the cylinder (container) $z'(-)$ is used. It means height $z(m)$ was divided by magnitude of container radius $R(m)$. Because of symmetry only half of the container section is displayed. Axis of symmetry is situated on the left of fig. 1. Contours of Lorentz forces are non-dimensional – normalized by maximum value of Lorentz forces. The range of Lorentz forces values is from zero to one.

Maxima of Lorentz forces in azimuthal direction are displayed by red colour, minima by blue colour. Maxima of these forces are occurred on the outer walls of cylinder in the half of container high. On the contrary minima of magnetic forces are in the axis of cylinder and on upper and lower base (based on boundary conditions).

III. LORENTZ FORCES IN THE CONTAINER IN CUBOID SHAPE

Input data for comparing Lorentz forces in the container with cuboid shape were obtained from the computing program NS-FEM3D which uses DDS method of computing. The

Delayed Detached Eddy Simulation model has been applied as a turbulent approach. This approach was implemented for higher Taylor number. Without any turbulent approach study of unsteady flows driven by magnetic field was limited only for lower Taylor number. Complete summary of applied mathematical model and validations see in [13].

The size of cuboid edge was chosen $2L = 0,03$ m. Database from this computing code were created by data matrix – coordinates of grid node points, values of Lorentz forces component (or more precisely form of accelerations) in the Cartesian coordinate system. And then this database was processed in software MathCad (version 15). In MathCad was created program for transformation forces in cylindrical coordinates. Only Lorentz forces in azimuthal direction was monitored. This part of Lorentz forces (azimuthal) is dominant. The grid of container was unstructured. Whole grid has over 2 200 000 elements.

Contours of Lorentz forces are displayed in central plane (it goes through vertical axis and it is perpendicular to lateral side of cuboid container. Because of unstructured grid weighting function was chosen. Lorentz force value in this central plane was determined by weighting function of four real grid points (the nearest point has the biggest weight, the most distant grid point has the lowest weight). For more details about this weighting function you can see to my earlier work [14].

Lorentz forces were divided by maximum value of the Lorentz forces before displaying in the central plane, so that contours of Lorentz forces are non-dimensional – normalized. The range of Lorentz forces values is from zero to one. The reason of normalizing forces is comparison Lorentz forces in cylindrical container and cuboid container.

A. Contours of Lorentz forces

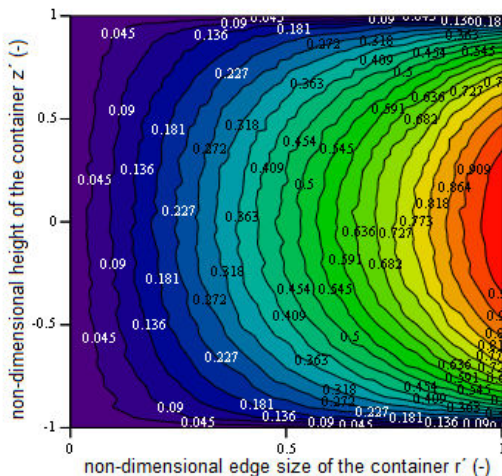


Fig. 2 Contours of time – averaged Lorentz forces in azimuthal direction for cuboid container

Fig. 2 shows contours of time – averaged Lorentz forces in azimuthal direction in the cuboid container. In horizontal axis non-dimensional cuboid edge size $r'(-)$ is used. That means cuboid edge size $r(m)$ was divided by magnitude of container

edge size $L(m)$. In vertical axis non-dimensional height of the container $z'(-)$ is used. That means height $z(m)$ was divided by magnitude of container edge size $L(m)$. Because of symmetry only half of the container section is displayed. Axis of symmetry is situated on the left of fig. 2.

IV. COMPARING LORENTZ FORCES IN CYLINDRICAL AND CUBOID CONTAINER

It is possible to compare Lorentz forces only based in fig. 1 and fig. 2. Maxima and minima are displayed in the same places, but values of Lorentz forces in the cuboid container are bigger than Lorentz forces in the cylindrical container. The shape of contours forces in cuboid container is flatter than contours in cylindrical container. Better comparing is displayed in fig. 3. In fig. 3 there are differences in values normalized Lorentz forces in cuboid container and cylindrical container.

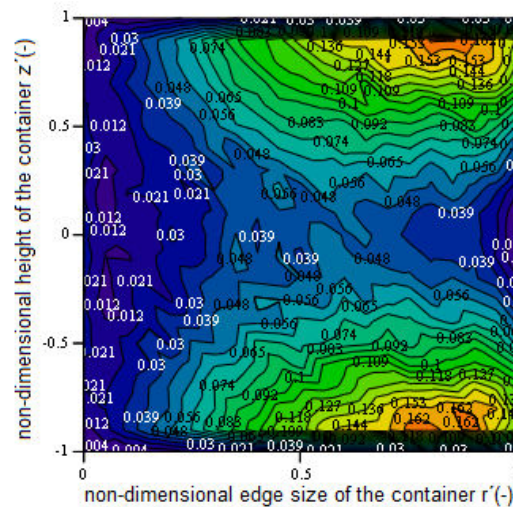
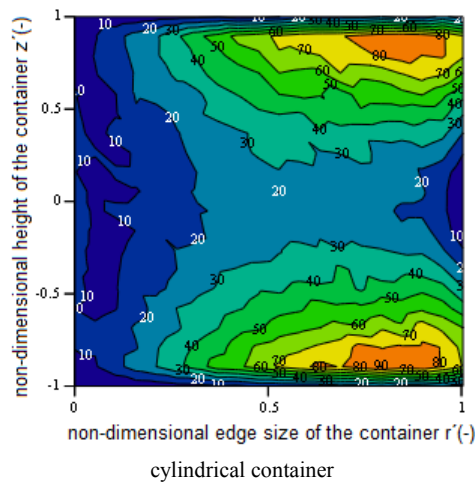


Fig. 3 Difference between Lorentz forces in cuboid and cylindrical container

In horizontal axis non-dimensional cuboid edge size $r'(-)$ is used as well. In vertical axis non-dimensional height of the container $z'(-)$ is used. Because of symmetry only half of the container section is displayed. Axis of symmetry is situated on the left of fig. 3.

Maxima of differences in values normalized Lorentz forces in cuboid container and cylindrical container are displayed by red colour, minima by blue colour. Maxima of these differences are occurred on the upper and lower base of the container near the outside walls. The maxima are caused by flatter shape contours in cuboid container than contours in cylindrical container. Higher values of Lorentz forces in cuboid container are apparently caused by shape of the container – container edges. Moving (dominantly in azimuthal direction) melt is accelerating and slowing owing to container edges and cross-section change.

Fig. 4 Percentage difference between Lorentz forces in cuboid and



In horizontal axis non-dimensional cuboid edge size $r'(-)$ is used as well. In vertical axis non-dimensional height of the container $z'(-)$ is used. Because of symmetry only half of the container section is displayed. Axis of symmetry is situated on the left of fig. 4.

In fig. 4 percentage difference between Lorentz forces in cuboid and cylindrical container is displayed. Referential value is maximum difference between forces in cuboid and cylindrical container. Percentage value of this difference is 100 %. Other values were divided by this maximum value. Resulting difference is displayed in percentage.

V. DEPENDENCE OF LORENTZ FORCES ON NON-DIMENSIONAL HEIGHT OF CONTAINER

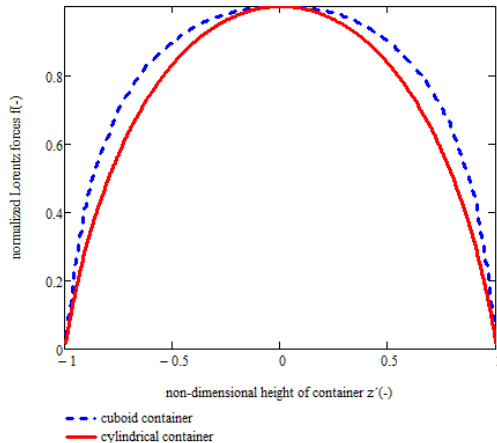


Fig. 5 Dependence of Lorentz forces on non-dimensional height of container

Dependence of time – averaged normalized Lorentz forces in azimuthal direction on non-dimensional height of container is displayed in fig. 5. Normalized Lorentz forces are in vertical axis and non-dimensional height of the container is in horizontal axis. Normalized Lorentz forces in cuboid container (from computing program NS-FEM3D) are displayed by blue dash line, forces in cylindrical container by red line. Lorentz force is a bivariate function (r and z). For displaying forces in

graph value of coordinate r was chosen on lateral surface of the container ($r' = r/R = 1$). Shape of this graph answers to contours of Lorentz forces in azimuthal direction (fig. 1 and fig. 2). Maxima of Lorentz forces are occurred on the outer walls of container in the distance $z' = 0$ (in half of container height). On the contrary minima (zero value of function) of magnetic forces are on upper and lower base (because of boundary conditions). Shapes of Lorentz forces contours in cuboid container are flatter than shape of forces contours in cylindrical container. This dependence corresponds to the published results of others authors, see [3, 4].

VI. CONCLUSIONS

My work will be proceed on change the whole determination system from cylindrical container to cuboid container. The aim is finding analytical formula for time-averaged Lorentz forces in azimuthal direction in cuboid container. This analytical formula is important for computing program NS-FEM3S. Results of analytical formula will be compared with the exact result of the computing program NS-FEM3D and finally integrated to another flow computing to speed up time of this code computing.

REFERENCES

- [1] P. A. Davidson: "An Introduction to Magnetohydrodynamics", Cambridge, 2001
- [2] P. Dold, K. W. Benz: "Rotating magnetic fields: fluid flow and crystal growth applications",
- [3] R. Mößner, G. Gerbeth: "Buoyant melt flows under the influence of steady and rotating magnetic fields", Journal of Crystal Growth, 1999
- [4] K.-H. Spitzer, "Application of Rotating Magnetic Fields in Czochralski Crystal Growth", Progress in Crystal Growth and Characterization of Materials 38, pp 39-58, 1999
- [5] L. M. Witkowski, J. S. Walker: "Flow driven by Marangoni convection and Rotating Magnetic Field in a Floating – Zone configuration", Magnetohydrodynamics, Vol. 37, 2001
- [6] E. Yildiz, S. Dost: "A numerical simulation study for the effect of magnetic fields in liquid phase diffusion growth of SiGe single crystals", Journal of Crystal Growth 291, 2006
- [7] Doležal I, Musil L.: "Modern industrial technologies based on processes in fluid metal controlled by electromagnetic field", Praha, 2003
- [8] K. Horáková, K. Fraňa: "Lorentz forces of rotating magnetic field", Mechanical Engineering Journal Strojárstvo, 2009, Slovak Republic
- [9] K. Horáková, K. Fraňa, "The effect of Lorentz forces parameters", Experimental fluid mechanics 2009, Liberec, Czech Republic
- [10] K. Fraňa, J. Stiller, "The Finite Element Method for Simulations of Magnetically Driven Flows", International journal of mathematics and computers in simulation, Issue 3, Vol. 1, 2007, pp. 300-306
- [11] J. Priede, "Theoretical study of a flow in an axisymmetric cavity of finite length driven by a rotating magnetic field", Ph.D. thesis, Institute of Physics, Latvian Academy of Science, Salaspils, 199
- [12] Marty PH.; L. Witkowski, "On the stability of rotating MHD Flows", Transfer Phenomena in Magnetohydrodynamic and Electroconducting Flows, 327-343, Netherlands, 1999
- [13] K. Fraňa, J. Stiller, A numerical study of flows driven by a rotating magnetic field in a square container, European Journal of Mechanics - B/Fluids, Issue 4, Vol. 27, 2008, p.p. 491-500
- [14] K. Horáková, K. Fraňa, "Energetic spectra of unsteady flows", Journal of Applied Science in the Thermodynamics and Fluid Mechanics, No. 1/2011